HIGH TEMPERATURE CREEP OF OXIDE-FIBRE/METAL-MATRIX COMPOSITES UNDER VARIABLE LOADING

S.T.Mileiko, V.M.Kiiko and K.A.Khvostunkov

Solid State Physics Institute of Russian Academy of Sciences, Chernogolovka Moscow distr., 142432 Russia

ABSTRACT

The present paper aims at testing a hypothesis of failing a relatively weak fibre/matrix interface under variable loading that yields an increase in steady state creep rate. The hypothesis is tested qualitatively by comparing the creep behaviour of composites with various interface strength values under the conditions mentioned. The hypothesis is tested semi-quantitatively by estimating the interface strength as a result of an event yielding an increase in creep rate. The latter needs to a usage of a microstructural creep model. Both approaches are used in the paper and the results support the hypothesis. Experimental data obtained are an additional argument to a necessity to develop metal matrix composites with a strong interface, which can be a base for real creep resistant composites with high temperature use.

1 INTRODUCTION

Heat resistant materials in jet engines are expected to undergone variable loading. This calls for systematic study of the material behaviour under such conditions. It seems to be particularly important for fibrous composites since it has been found in creep experiments [1], in which oxide-fibre/nickel-based-matrix composites are undergone to loads variable with time, that low-cycling loading can yield a decrease in the fibre/matrix interface strength, which leads to an increase in the creep rate. Such behaviour is characteristic for composites with fairly low interface strength. On the same time, it is clear [2,3] that increasing the interface strength yields an essential increase in creep resistance of a composite. On the other hand, a sufficiently weak interface can in some cases provide an additional contribution to fatigue resistance of a composite (see Chapter 7 in Ref. [4]). All this calls for a scrupulous study of behaviour of the fibre/matrix interface in a composite under variable loading.

Obviously, a rather vast variety of both composite microstructures and possible paths of loading and heating can produce such a volume of experimental information that can be appropriately systematised and understood only if an adequate model of a composite with a fibre/matrix interface that can be changing as a result of loading and straining is available. Moreover, in such case a possibility of an optimisation of the microstructure of a composite can be visible.

The present paper focuses on a model of the interface, which actually is a further development of the model published recently [2]. The development is based on experimental observations.

2 EXPERIMENTAL

Creep experiments with various composites reinforced with oxide fibres, which are characterised by different interface strength values, have yielded definite dependencies between the interface strength and creep resistance of composites [2,5,6]. This allows avoiding measurements of the interface strength in the present work.

2.1 MATERIALS

The present experiments were conducted with composites reinforced with sapphire fibres and a variety of the matrices that provided various interface strength values. The high interface strength is reached in composites with TiAl-based matrix; the interface strength in composites with Ni- and Ni_3Al-based matrices can be controlled (see, e.g. [2,5,7,8,9]).

Two materials as the matrices were alloys based on Ni_3Al. The first one was also used in Ref. [5]. The second alloy differs from the first one just by an additional alloying to increase slightly the interface strength. The third matrix was titanium aluminide (Ti-48Al) as described in Ref. [6]. Fabrication process of the composite specimens are disclosed elsewhere [6,???]. The chemical composition and microstructure of the composites are not important for the purposes of the present study and they can be found in the above references as well. Some characteristics of the specimens, which are necessary to calculate creep properties of the composites, are given in Table 1.

All specimens were tested in bending. Original experimental data were then used to calculate tensile creep characteristics according to a procedure described in details in Ref. [2]. A feature of the testing procedure to be mentioned here is a somewhat non-standard way to measure specimen displacement that includes an additional value to a real displacement on the transient stage of a creep curve; hence, steady state creep rate is the only reliable value measured in the tests. The reliability of this value is proved by direct measurements of the specimen displacement in parallel to the non-standard method mentioned, Fig. 1.

Table 1. Description of the specimens tested.

Specimen number	Matrix material	Fibre volume fraction	Specimen's diameter	Distance between supports	Characteristic load	Maximum initial bending stress	Characteristic creep rate
			mm	mm	N	MPa	h^{-1}
A1446	Ni_3Al-1	0.22	4.0	42	108	180.1	0.37
					59	98.2	6.57×10^{-3}
A1642	Ni_3Al-1	0.20	4.4	50	49	73.2	8.95×10^{-4}
A1684	Ni_3Al-2	0.41	4.6	46	49	59.0	1.17×10^{-5}
A1685	Ni_3Al-2	0.41	4.6	46	78.4	94.3	1.92×10^{-3}
A1651	Ti-48Al	0.22	4.67	42	255		
A1655	Ti-48Al	0.22	4.51	38	255		

2.2 ORIGINAL CREEP CURVES

Typical creep curves at variable loading are presented in Fig. 1 to Fig. 4. Rates of the specimen displacement versus loading stage for two specimens characterized in Fig. 1 are plotted in Fig. 5. The following observations of the creep behaviour of composites with different values of the interface strength are worth to be noted.

Composites with a weak interface change their creep characteristics after unloading and subsequent loading (Fig. 1 to Fig. 3) certainly as a result of interface damage. Creep rate after such a cycle increases essentially.

The damage depends on the amplitude of loading/unloading cycle as can be clearly seen in Fig. 5.

Composites with a strong interface are not undergone severe interface damage – compare Fig. 3 and Fig. 4. Under low cycling conditions, the composites can be considered as structurally stable materials, Fig. 6.

3 MODELLING OF THE CREEP BEHAVIOUR

We start with a further development of a recently published model of creep behaviour of brittle-fibre/creeping-matrix composites [2] to interpret experimental data described in Section 2.2 and then proceed with a model of the interface fracturing under low-cycle loading.

3.1 FURTHER DEVELOPMENT OF A CREEP MODEL

A simple model of creep of a composite with a brittle fibre and creeping matrix was suggested by one of the author in Ref. [2]. The behaviour of an elastic fibre follows the Weibull strength distribution, so we have the scale dependence for the fibre as

$$\sigma_*^{(f)}(l) = \sigma_o^{(f)}(l_o)\left(\frac{l}{l_o}\right)^{-\frac{1}{\beta}}, \tag{1}$$

where $\sigma_o^{(f)}(l_o)$ is the average strength of a fibre of a length l_o, and β is exponent in the Weibull distribution.

Let the creep law of the matrix will be

$$\dot{\varepsilon} = \eta_m\left(\frac{\sigma}{\sigma_m}\right)^m, \tag{2}$$

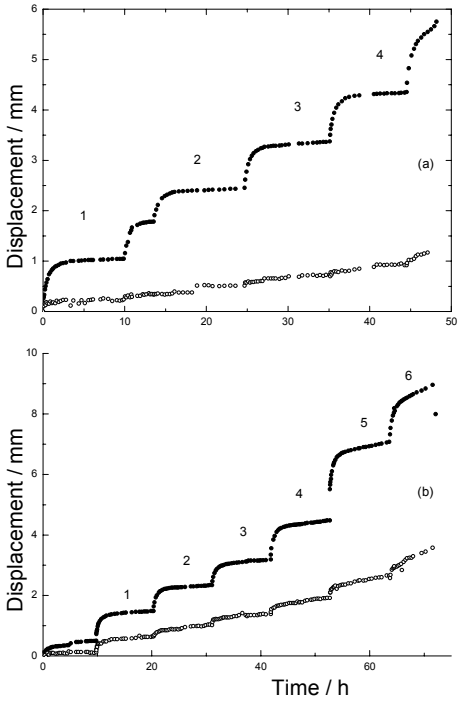

Fig. 1. Displacement at the specimen centre versus time for specimens a1685 (a) and a1685 (b) at temperature 1150°C. The matrix is alloy 2. The testing was going on for about 10 h, and then a specimen was unloaded and cooled. After about 12 h testing started again. On stages 1 to 6 marked by numbers in the graph field, at $t > 10$ h, the load was 78.4 N. Open points were obtained by direct measurements, solid points present real creep curves on the steady-state stage only.

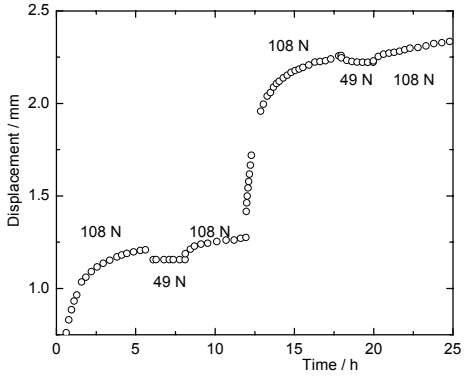

Fig. 2. Displacement at the specimen centre versus time for a specimen with sapphire fibre and alloy 1 based on Ni_3Al as a matrix at temperature 1150oC and load Q = 108 - 49 N. The test was interrupted at t = 12.2 h for about 12 h.

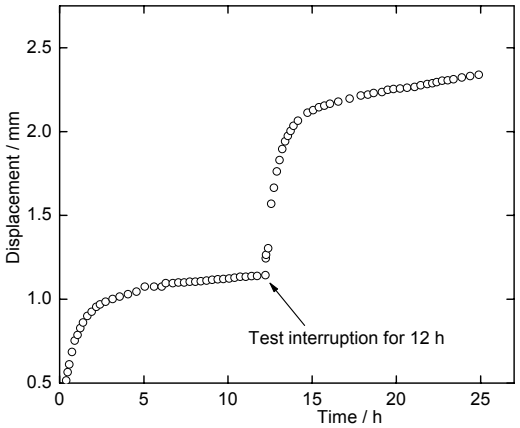

Fig. 3. Displacement at the specimen centre versus time for specimen (the matrix is alloy 1) at temperature 1150°C and load $Q = 49$ N.

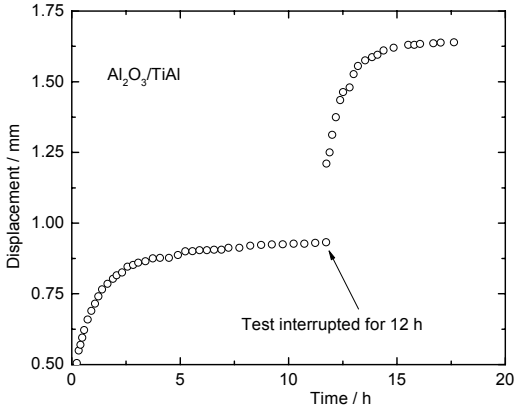

Fig. 4. Displacement at the specimen centre versus time for specimen a1651 (TiAl matrix) at temperature 900°C and load $Q = 255$ N.

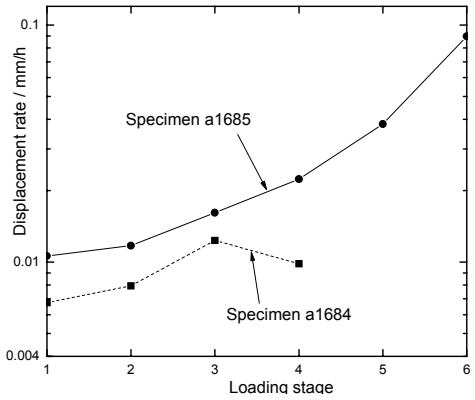

Fig. 5. Steady state displacement rate of the specimen, curve of which is shown in Fig. 1.

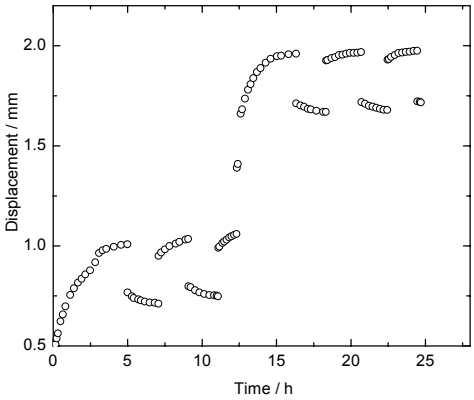

Fig. 6. Displacement at the specimen centre versus time for specimen a1655 (titanium-aluminide matrix) at temperature 900°C and load Q = 255 – 29 N. At t = 12.3 h the specimen was unloaded and cooled. After about 12 h testing started again.

where η_m, σ_m, and m are constants, one of which can be chosen arbitrarily, so in what follows we take $\eta_m = 10^{-4}$ h^{-1}.

Then the dependence between creep strain rate of the composite and composite stress is obtained [2] as

$$\sigma = \lambda\sigma_m\left[\left(\frac{\sigma_o^{(f)}}{\lambda\sigma_m}\right)^{\beta}\left(\frac{l_o}{d}\right)\right]^{\frac{m+1}{n}}\left(\frac{\dot{\varepsilon}}{\eta_m}\right)^{\frac{1}{n}}V_f + \sigma_m\left(\frac{\dot{\varepsilon}}{\eta_m}\right)^{\frac{1}{m}}V_m \ . \qquad (3)$$

Here d is a characteristic cross-section size of the fibre, $n = m + \beta + m\beta$ and

$$\lambda = \alpha\Phi(m) \qquad (4)$$

where α is a continuity coefficient of the fibre/matrix interface; α = 0 if there is no adhesion, α = 1 if the interface is continuous and the adhesion is ideal that means that the interface strength is no less than the matrix strength;

$$\Phi(m) = \left(\frac{2}{3}\right)^{\frac{1}{m}}\left(\frac{m}{2m+1}\right)\left[\left(\frac{2\sqrt{3}}{\pi}\right)^{-\frac{1}{2}} - 1\right]^{-\frac{1}{m}}$$

is a geometrical factor.

It is convenient to rewrite Eq. (3) as

$$\sigma = \sigma_m\left\{\alpha^{\frac{m}{n}}\Psi\left(\frac{\dot{\varepsilon}}{\eta_m}\right)^{\frac{1}{n}}V_f + \left(\frac{\dot{\varepsilon}}{\eta_m}\right)^{\frac{1}{m}}V_m\right\}, \qquad (5)$$

where

$$\Psi = \Phi(m)\left[\left(\frac{\sigma_o^{(f)}}{\sigma_m}\right)^{\beta}\left(\frac{l_o}{d}\right)\right]^{\frac{m+1}{n}} .$$

If a cycling loading (or actually other effect) yields a decrease of the interface strength, it can be treated as a decrease in the value of α, which causes an increase in the creep rate at a fixed value of stress σ. Let the original values of continuity factor and steady state creep rate will be α_1 и $\dot{\varepsilon}_1$, respectively, and

their value after unloading and subsequent loading will be $\alpha_2 = \xi\alpha_1$ и $\dot{\varepsilon}_2 = \chi\dot{\varepsilon}_1$. Equating values of σ given by Eq. (5) for two sets of the values of α и $\dot{\varepsilon}$ yields

$$\xi = \left\{ \chi^{-\frac{1}{n}} \left[1 - \left(1 - \chi^{\frac{1}{m}} \right) \left(\frac{\dot{\varepsilon}_1}{\eta_m} \right)^{\frac{n-m}{nm}} \frac{V_m}{V_f} \frac{\alpha_1^{-\frac{m}{n}}}{\Psi} \right] \right\}^{\frac{n}{m}} \tag{6}$$

Equation(6) allows evaluating a change in the interface strength, ξ, if its original value, α_1, is known and a new value of the creep rate has been measured. The expression obtained can be directly applied to results of the tensile tests.

Results of bending tests, which are used in the present series of the work as an express method of measuring creep characteristics of composites, cannot be analysed in such a simple way. Hence, the following simplified analysis yields a rough estimation. Actually, the whole analysis of the bending tests to obtain tensile creep characteristics is an approximate one [2]. In such analysis, the creep law is assumed to be the same for tension and compression similar to that given by Eq. (2) with constants $\eta_n = 10^{-4}\,\text{h}^{-1}$, σ_n and n; σ_n is a stress to cause the creep strain 10^{-2} for 100 h. The rate of displacement in the centre of a specimen is [2]

$$\dot{f} = \eta_n \frac{L}{2^{2(n+1)}(n+2)\mu(n)} \left(\frac{Q}{\sigma_n R^2} \right)^n \left(\frac{L}{R} \right)^{n+1}, \tag{7}$$

where L and R are the distance between the supports and specimen radius, respectively.

Obviously,

$$\frac{\dot{f}_1}{\dot{f}_2} = \left[\frac{\sigma_{n1}}{\sigma_{n2}} \right]^{-n}, \tag{8}$$

where indexes 1 and 2 distinguish the original values and those after the first unloading/loading cycle. Using Eq. (3) yields the following expression analogous to Eq. (6):

$$\alpha_2 = \alpha_1 \varsigma^{1/n} - \frac{V_m}{\Psi V_f} \left(1 - \varsigma^{1/n} \right) \tag{9}$$

Here

$$\zeta = \left(\frac{\dot{f}_1}{\dot{f}_2} \right).$$

3.2 SYSTEMATISATION AND INTERPRETATION OF EXPERIMENTAL DATA

As noted in Section 2.2, the effect of cycling depends on "amplitude" of cycling, although this statement is rather qualitative since a value of the amplitude cannot be measured in bending. Hence, in Table 1 there are shown values of a maximum creep rate at the first stage of loading calculated for a point of a specimen where the tensile stress reaches a maximum (characteristic creep rate). They are assumed to be a measure of the cycling amplitude.

The matrix alloys used to make composites provide, under accepted technological parameters, different values of α. In composites with Ni_3Al-based matrices the strength of the interface is low, Table 2. Let us call the interface in composites with alloy 1 as "*weakest*", in those with alloy 2 as "*weak*", and those with TiAl matrix as "*ideal*".

Table 2. Interface strength and creep resistance of the composites.

Matrix alloy	α	Temperature	Tensile stress to cause 1% of creep strain for 100 h
		°C	MPa
Ni_3Al-1	0.005	1150	50-55 at $V_f = 0.2 – 0.4$ [1]
Ni_3Al-2	0.05	1150	65-70 at $V_f = 0.2 – 0.4$
TiAl	1	900	200 at $V_f = 0.20 – 0.25$

The weakest interface

The complete unloading of specimen a1642 yields (Fig. 3), after restoring the load, the displacement rate corresponding to $\alpha = 0$ according to Eq. (9). A partial unloading (specimen a1446 - Fig. 4) and subsequent loading to the initial value yields some increase in the displacement rate (stage 3 as compared to stage 1); the complete unloading yields an essential increase in the displacement rate (stage 5). The next partial unloading – reloading cycle (stages 5 - 6) does not lead to an increase in the creep rate, perhaps due to a stabilisation of a microstructure with a completely destroyed interface.

The weak interface

Two specimens of this type (a1684 and a1685 in Table 1) were tested. Specimen a1684 had a characteristic creep rate of about 10^{-5} h^{-1}; specimen a1685 had a characteristic creep rate two orders of the magnitudes higher. Let us consider the results presented in Fig. 1 and Fig. 5 on the background of the creep model. Parameters of the model accepted earlier while analysing the creep behaviour of these composites under a constant loading are given in Table 3. Using Eq. (9) yields values of α for a series of loading stages presented in Fig. 7.

The ideal *interface*

A special discussion of the behaviour of composites with the ideal interface (Fig. 4 and Fig. 6) is not necessary since it is not differ from that qualitatively from that of structurally stable materials. Cyclic loading, at least under the conditions fulfilled in the present series of experiments, does not affect the interface.

Table 3. Parameters of the creep model.

Fibre				Matrix		Interface
$\sigma_o^{(f)}$	β	l_o	d	σ_m	m	α
MPa		mm	mm	MPa		
150	3	1	0.1	41	5.4	0.005 Ni_3Al-1 [1]
						0.05 Ni_3Al-2

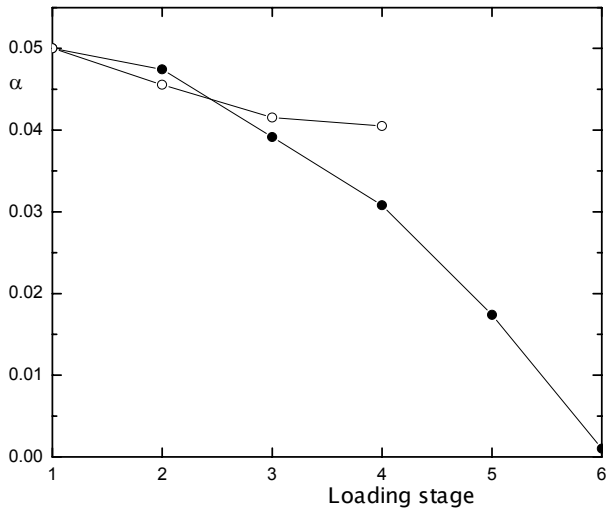

Fig. 7. Interface strength versus loading stage number for specimens described in Fig. 1 and Fig. 5. Open and solid points stand for specimen a1684 and a1685, respectively.

3.3 A MODEL OF THE INTERFACE

Let us consider again 3-poin bending of a circular composite rod of radius R under creep conditions. Let the composite obeys creep law given by Eq. (3) under tension and compression, the latter being a rough assumption to simplify a solution. Then creep rate at a point with coordinate y, the distance from the neutral axis, will be

$$\dot{\varepsilon} = \kappa(x) y \,. \tag{10}$$

where x is the coordinate along the rod length and κ is the rate of curvature increase.
Combining Eqs. (3) and (10) yields

$$\sigma = K_f \alpha^{\frac{m}{n}} \dot{\varepsilon}^{\frac{1}{n}} + K_m \dot{\varepsilon}^{\frac{1}{m}} \tag{11}$$

where constants K_f and K_m are easily expressed.
Applied bending moment is

$$M(x) = Q\frac{x}{2}$$

where Q is the applied load. The moment caused by the stresses is

$$M(x) = 4\int_0^R \left(K_f \alpha^{\frac{m}{n}} (\kappa y)^{\frac{1}{n}} + K_m (\kappa y)^{\frac{1}{m}} \right) \sqrt{R^2 - y^2}\, y dy = 4K_f I(n) \alpha^{\frac{m}{n}} \kappa^{\frac{1}{n}} + 4K_m I(m) \kappa^{\frac{1}{m}} \tag{12}$$

Here

$$I(n) = \int_0^1 t^{\frac{1}{2n}} \sqrt{1-t}\, dt$$

Consider a simple case when a contribution of the matrix can be neglected. In this case, Eq. (12) can be written as

$$M(x) = 2R^{\left(3+\frac{1}{n}\right)} \kappa^{\frac{1}{n}} K_f \alpha^{\frac{m}{n}} I(n) \tag{13}$$

and

$$\kappa = \left(\frac{Qx}{4R^{\left(3+\frac{1}{n}\right)} K_f \alpha^{\frac{m}{n}} I(n)} \right)^n$$

Mohr's formula [10] yields

$$\dot{f}\left(\frac{L}{2}\right) = \int_0^{\frac{L}{2}} \kappa \frac{x}{2} dx = \frac{1}{\alpha^m} \left(\frac{P}{\left(K_f I(n)\right)} \right)^n \frac{L^{n+2}}{R^{(3n+1)} 2^{3n+3} (n+2)} \tag{14}$$

where L is the distance between supports.
Let us assume that the total length a of discontinuity on the interface depends on number of cycle N according the Paris law [11]

$$N = \frac{1}{CY^2 \sigma^2 \pi} \ln \frac{a}{a_0} \tag{15}$$

Here C and Y are constants, a_o is the initial value of discontinuity, $a = 1 - \alpha$. Hence

$$\alpha = 1 - (1 - \alpha_0) \exp\left(N K_2 \sigma^2\right) \tag{16}$$

where $K_2 = \pi C Y^2$. The specimen ruptures at the value of N corresponding $\alpha = 0$. Replacing Q with σ yields just a change in dimension of constant K_2. Let a new constant be K_p. Eqs. (14) and (16) lead to the dependence of the rate of displacement on the stage of loading

$$\dot{f}\left(\frac{L}{2}\right) = \left(\frac{Q}{4R^{\left(3+\frac{1}{n}\right)} K_f \left[1 - (1-\alpha_0)\exp(N K_P Q^2)\right]^{\frac{m}{n}} I(n)} \right)^n \frac{L^{n+2}}{2^{n+2}(n+2)} \tag{17}$$

Here

$$K_P = \frac{1}{NQ^2}\ln\left[\left(1-\left[\frac{Q}{4R^{\left(3+\frac{1}{n}\right)}K_f I\left[\frac{2^{n+2}(n+2)}{L^{n+2}}\dot{f}\left(\frac{L}{2}\right)\right]^{\frac{1}{n}}}\right]^{\frac{n}{m}}\right)(1-\alpha_0)^{-1}\right].$$

An example of calculated dependencies of α on N is given in Fig. 8.

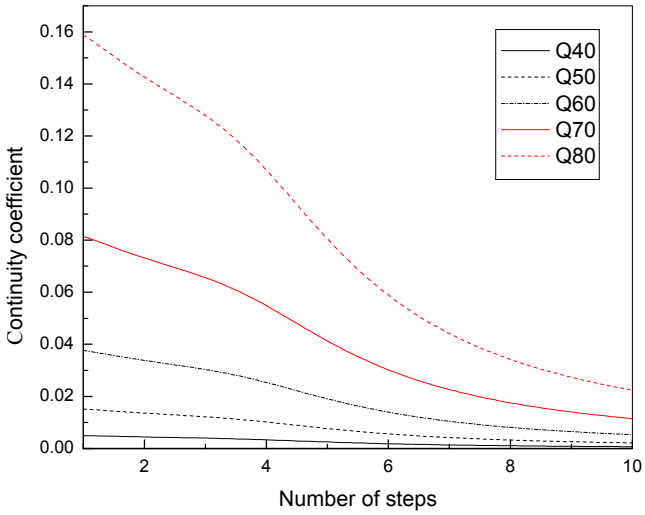

Fig. 8. Dependencies of continuity coefficient α on number N of cycles for various applied loads written as QXX where XX is the load in Newtons. The values of constants are $L = 40$ mm, $R = 2.5$ mm, $n = 15$, $m = 3$.

4 CONCLUSIONS

1. Low-cycle loading under high-temperature creep of composites with the *ideal* interface does not yield the interface failure. The creep behaviour of such composites does not differ from that of microstructurally stable materials: the steady-state creep rate does not depend of pre-history of loading.
2. A weak interface (α ≤ 0.05) is failing under the conditions of low-cycle loading, the process rate is certainly dependent on both values of α and loading amplitude (characteristic creep rate).
3. A creep model suggested earlier is now developed to take into account the interface failuring during cycling loading.
4. Experimental data presented are an additional argument in favour of developing oxide-fibre/metal-matrix composites with high interface strength.
5. On the same time these data show a necessity to study the behaviour of composites with island-like interface, an example being ceramic matrix composites with porous matrix, under cycling loading.

ACKNOWLEDGEMENTS

The work was supported by Russian Foundation for Basic Research (Projects # 02-01-00502 and # 02-01-00442) and International Science and Technology Centre (Project # 2456). The authors are thankful to their colleagues, Mr A.A. Kolchin, Dr V.P. Korzhov, and Mr A.Ya. Mizkevich for their help in the experimental work.

1 **Mileiko, S.T.** and **Kiiko**, **V.M.,** High temperature creep of metal matrix composites under variable loadings, *Mechanics of Composite Materials* (in Russian), in press.

2 **Mileiko, S.T.**, Oxide-fibre/Ni-based matrix composites – III: A creep model and analysis of experimental data, C*ompos. Sci. and Technol.,* **62**/2 (2002), 195-204.
3 **Mileiko, S.T., Sarkissyan, N.S., Kolchin, A.A., Kiiko**, **V.M.,** Oxide fibres in a Ni-based matrix – do they degrade or become stronger? *Journal of Materials: Design and Applications* (in press).
4 **Mileiko,S.T**. *Metal and Ceramic Based Composites*, Elsevier, Amsterdam, 1997.
5 **Mileiko, S.T., Kiiko**, **V.M., Kolchin, A.A., Korzhov**, **V.P.** and **Prokopenko**, **V.M**., Oxide-fibre/Ni-based matrix composites – II: Mechanical behaviour, C*ompos. Sci. and Technol.,* **62**/2 (2002) 181-193.
6 **Mileiko, S.T., Povarova, K.B., Serebryakov, A.V., Korzhov**, **V.P., Kolchin, A.A., Kiiko**, **V.M., Starostin, M.Yu., Sarkissyan, N.S.** and **Antonova**, **A.V.,** High temperature creep properties of sapphire-fibre/titanium-aluminide-matrix composites, *Scripta Materialia,* **44**/10 (2001) 2463-2469.
7 **Tewari, S.N, Asthana, R.,** and **Noebe, R.D**., Interfacial shear strength of cast and directionally solidified NiAl-Sapphire fibre composites. *Met Trans* **24A** (1993) 2119-2125.
8 **Asthana,R., Tiwari,R.**, and **Tewari,S.N.**, Influence of Cr and W alloying on nterfacial shear strength of cast and directionally solidified sapphire NiAl composites, *Metall. Mater. Trans*. **26A** (1995) 2175-2184.
9 **Tewari,S.N., Asthana,R., Tiwari,R., Bowman,R.R.**, and **Smith,J.,** Influence of interfacial reactions on fiber-matrix interfacial shear strength in sapphire fiber-reinforced NiAl(Yb) composites, *Metall. Mater. Trans*. **26A** (1995) 477-491.
10 **Rabotnov,Yu.N**. and **Mileiko,S.T.**, *Short-Time Creep*, Nauka Publishers, Moscow, 1970 (in Russian).
11 **Suresh, S**., *Fatigue of Materials*, Cambridge University Press, 1991.